Smart Structures and Systems, *Vol. 30, No. 1 (2022) 75-88*
https://doi.org/10.12989/sss.2022.30.1.075

A generalized adaptive variational mode decomposition method for nonstationary signals with mode overlapped components

Jing-Liang Liu*[1,2], Fu-Lian Qiu [1a], Zhi-Ping Lin [3b], Yu-Zu Li [1c] and Fei-Yu Liao [1,2d]

[1] *College of Transportation and Civil Engineering, Fujian Agriculture and Forestry University, Fuzhou 350002, China*
[2] *"Digital Fujian" Laboratory of Internet Things for Intelligent Transportation Technology, Fuzhou 350002, China*
[3] *Fujian Expressway Group Co., LTD, Fuzhou 350001, China*

(*Received April 30, 2021, Revised April 2, 2022, Accepted April 28, 2022*)

Abstract. Engineering structures in operation essentially belong to time-varying or nonlinear structures and the resultant response signals are usually non-stationary. For such time-varying structures, it is of great importance to extract time-dependent dynamic parameters from non-stationary response signals, which benefits structural health monitoring, safety assessment and vibration control. However, various traditional signal processing methods are unable to extract the embedded meaningful information. As a newly developed technique, variational mode decomposition (VMD) shows its superiority on signal decomposition, however, it still suffers two main problems. The foremost problem is that the number of modal components is required to be defined in advance. Another problem needs to be addressed is that VMD cannot effectively separate non-stationary signals composed of closely spaced or overlapped modes. As such, a new method named generalized adaptive variational modal decomposition (GAVMD) is proposed. In this new method, the number of component signals is adaptively estimated by an index of mean frequency, while the generalized demodulation algorithm is introduced to yield a generalized VMD that can decompose mode overlapped signals successfully. After that, synchrosqueezing wavelet transform (SWT) is applied to extract instantaneous frequencies (IFs) of the decomposed mono-component signals. To verify the validity and accuracy of the proposed method, three numerical examples and a steel cable with time-varying tension force are investigated. The results demonstrate that the proposed GAVMD method can decompose the multi-component signal with overlapped modes well and its combination with SWT enables a successful IF extraction of each individual component.

Keywords: adaptive; closely-spaced; instantaneous frequency; mode overlapped; variational modal decomposition

1. Introduction

Practical engineering structures in operation are essentially time-varying or nonlinear structures when exposed to service loads or extreme loads (Liu *et al*. 2015). The resultant response signals of such time-varying structures are non-stationary, closely-spaced and even mode overlapped at some cases (Le and Caracoglia 2015). For these non-stationary signals, conventional time or frequency domain signal processing techniques can only capture their features in time or frequency domain alone, without revealing intrinsic characters in both time and frequency domains simultaneously (Cempel and Tabaszewski 2007). In contrast, time frequency analysis (TFA) is potential to trace internal features of non-stationary signals in a joint time-frequency domain and have attracted increasing attentions in the area of parameter identification (Feng *et al*. 2020). However, they still suffer some shortcomings. For example, linear time-frequency analysis, including short time Fourier transform and continuous wavelet transform, is essentially an integral transform with predefined basis and hence has limited time-frequency resolution due to the restriction of Heisenberg uncertainty principle. Bilinear TFRs such as Wigner-Ville distribution have the potential to provide good time frequency representations for multi-component signals, but they suffer outer interferences due to cross terms between multi-components (Lee *et al*. 2001). In order to enhance the time frequency readability of traditional TFAs, reassignment methods are developed by reallocating diluted energy (Auger and Flandrin 1995). For instance, synchrosqueezing wavelet transform (SWT) reassigns the energy in the frequency direction and hence suppresses the blur along the frequency axis (Daubechies *et al*. 2011, Thakur *et al*. 2013, Clausel *et al*. 2015, Oberlin *et al*. 2015). On a basis of SWT, a generalized synchro-squeezing transform approach is proposed by Li and Liang (2012) to reduce the diffusion in both time and frequency dimensions for frequency modulated (FM) signals. However, these post-processing methods cannot work well or even fail when the components of non-stationary signals are closely spaced or overlapped. Therefore, how to decompose a non-stationary signal with several closely spaced or overlapped mono-components successfully is highlighted and hence becomes the foremost issue to be

*Corresponding author, Ph.D.,
E-mail: liujingliang@fafu.edu.cn
[a] Graduate Student, E-mail: qfl_77@163.com
[b] Ph.D., E-mail: lzpgsgl@126.com
[c] Graduate Student, E-mail: lyz792756045@163.com
[d] Professor, E-mail: feiyu.liao@fafu.edu.cn

ISSN: 1738-1584 (Print), 1738-1991 (Online)

addressed.

As an iterative numerical approximation algorithm, empirical mode decomposition (EMD) is designed to decompose a multi-component signal into several intrinsic mode functions (IMFs) in a frequency order from high to low by cubic spline interpolation (Huang *et al*. 1998). However, it still has some drawbacks such as the lack of mathematical formulation, susceptibility to mode mixing under singularities and etc. (Feng *et al*. 2020, Poon and Chang 2007). To solve the mode mixing problem in EMD, a new algorithm named ensemble empirical mode decomposition (EEMD) is presented by injecting a generated white noise into the original signal. Owing to the injection of the additional white noise, EEMD probably separates closely-spaced components, but the corresponding calculation amount in turn increases (Liu *et al*. 2018). Furthermore, the signal decomposition results by EEMD are sensitive to parameter selection, even pseudo components may be produced if improper parameters are selected (Chen and Cui 2016). In addition to EMD-based algorithms, the local mean decomposition (LMD) method is developed by Smith (2005). LMD is essentially a self-adaptive algorithm to decompose an amplitude demodulated and frequency demodulated (AM-FM) signal into a small set of product functions, each of which is the product of an envelope signal and a FM signal (Smith 2005). Although LMD avoids the limitation of negative frequencies, the problems of end effect and mode mixing remain unsettled. The Hilbert vibration decomposition (HVD) presented by Feldman (2006) is potential to exploit the AM-FM property of IMFs, however, it is quite sensitive to background noises. Unlike HVD, a new algorithm called analytical mode decomposition (AMD) is developed by Chen and Wang (2012). The essence of the AMD theorem is the exact separation of a general time series into two functions whose Fourier spectrum are non-vanishing over two mutually-exclusive frequency ranges separated by a constant bisecting frequency. Despite the good performance of AMD on multi-component signal decomposition, its bisecting frequency is selected artificially based on the peak of the Fourier spectrum. Therefore, AMD is regarded as a subjective method to an extent. Recently, variational mode decomposition (VMD) is developed by Dragomiretskiy and Zosso (2014) to separate a multi-component signal into several band-limited IMFs. Due to its strong relations to the Wiener filter, VMD exhibits good robustness in processing noisy signals (Zhu *et al*. 2015). The superiority of VMD in processing certain types of signals has been demonstrated in various fields (Bagheri *et al*. 2018, Mohanty *et al*. 2014). For example, VMD is used as a multi-resolution technique in electrocardiograph signals to overcome some shortcomings of EMD (Lahmiri 2014). Isham *et al*. (2018) proposed a mode determination method for VMD by taking the advantages of similarity concept between the sum of variational mode functions and the input signal. This method is able to provide an accurate number of modes for response signals on condition that the input signal is known beforehand. Unfortunately, this prerequisite is often unsatisfied in practical civil engineering.

Although VMD behaves well on signal decomposition, it still suffers a problem that cannot be settled by the general frequency domain segmentation. That is to say, the number of modal components requires to be predefined for VMD (Dragomiretskiy and Zosso 2014). Another issue needs to be addressed is VMD cannot separate response signals composed of closely-spaced or overlapped modes effectively (Chen *et al*. 2019). The reason for this problematic issue is VMD shares a filter bank property similar to EMD, and therefore is subject to a narrow band assumption that the frequencies of component signals are required to be near constant. This property results in that VMD is only suitable for processing signals without overlapped modes, e.g., those signals composed of almost constant frequencies. However, when the modal frequencies of signals vary excessively over time and overlap with each other in frequency domain, VMD no longer performs satisfactorily (Feng *et al*. 2020). In view of these two problems mentioned above, a new method called generalized adaptive variational mode decomposition (GAVMD) is proposed in this paper. In this method, the number of component signals is adaptively determined at first by an index of mean frequency. Then, a generalized demodulation method is introduced to yield a generalized VMD algorithm that can decompose mode overlapped response signals successfully. With a use of GAVMD, the energy of the decomposed component signals concentrates around several curves on the time-frequency plane (Liu *et al*. 2018). After that, synchrosqueezing wavelet transform (SWT) is used to extract instantaneous frequencies (IFs) of the decomposed mono-component signals. The validity and accuracy of the proposed method are verified by three numerical examples and a steel cable with time-varying tension force. The results demonstrate that the proposed GAVMD can decompose multi-component signals with overlapped modes into several mono-components accurately and its combination with SWT enables a successful IF extraction of each decomposed component as well.

Hereafter, this paper is organized as follows. The principle of VMD is revisited in Section 2. The proposed GAVMD is detailed in Section 3. Three numerical case studies are employed in Section 4 to illustrate the proposed method, while an experimental case of a steel cable with time-varying tension force is investigated in Section 5. Conclusions are drawn in Section 6.

2. Variational mode decomposition

As a newly developed method for signal processing, VMD is capable of reducing the non-stationarity of time series with high complexity and strong nonlinearity, which makes it appropriate for non-stationary signal decomposition (Dragomiretskiy and Zosso 2014). Compared with EMD, VMD has a more solid mathematical theoretical foundation and overcomes some shortcomings of EMD based methods as well. However, it cannot separate closely spaced or mode overlapped components effectively, which hinders its application on practical engineering structures.

Typically, a multi-component signal usually consists of several components and each one is guaranteed to be a modal component with central frequency and finite bandwidth. Thereby, a multi-component signal can be expressed as the sum of several component signals and a residual.

$$x(t) = \sum_{q=1}^{Q} x_q(t) + r(t) \tag{1}$$

where $x_q(t) = A_q(t)\cos[\phi_q(t)]$ and each component is compact around a center frequency. $r(t)$ represents noise or observation error. Q denotes the total number of components or sub-signals, while q indicates an arbitrary component of the multi-component signals, that is to say, $q = 1, 2, \ldots, Q$.

In order to determine the center frequency and bandwidth of each component signal, a variational problem is constructed as Eq. (2). Under the premise that the sum of all modal component equals the original multi-component signal, the variational problem is transformed into a search of the modal function that minimizes the sum of the estimated bandwidths.

$$\min_{\{u_q\},\{\omega_q\}} \left\{ \sum_q \left\| \partial_t \left[\left(\delta(t) + \frac{j}{\pi t} \right) * u_q(t) \right] e^{-j\omega_q t} \right\|_2^2 \right\} \tag{2}$$

where $\{u_q\}$ and $\{\omega_q\}$ represent the q-th modal component and center frequency, respectively. $\delta(t)$ denotes the Dirac function, while $*$ represents the convolution operator.

In fact, Eq. (2) can be solved by combining quadratic penalty and Lagrange multiplication operator. As a classic way to encourage reconstruction fidelity, the quadratic penalty function behaves well in the presence of additive Gaussian noise. On the other hand, Lagrangian multiplication operator is exactly a common way of enforcing constraints strictly. Therefore, the combination of these two terms benefits both from the sound convergence characteristics of the quadratic penalty at the finite weight and the strict enforcement of the constraint by the Lagrangian multiplication operator (Dragomiretskiy and Zosso 2014). Since the Lagrange multiplication operator λ transforms the constrained variational problem into an unconstrained variational problem, the augmented Lagrange $\mathcal{L}$ is then introduced and shown in Eq. (3).

$$\begin{aligned} &\mathcal{L}(\{u_q\},\{\omega_q\},\lambda) \\ &= \alpha \sum_q \left\| \partial_t \left[\left(\delta(t) + \frac{j}{\pi t} \right) * u_q(t) \right] e^{-j\omega_q t} \right\|_2^2 \\ &\quad + \left\| x(t) - \sum_q u_q(t) \right\|_2^2 + \langle \lambda(t), x(t) - \sum_q u_q(t) \rangle \end{aligned} \tag{3}$$

where α is the quadratic penalty factor.

Actually, the original minimization problem as illustrated in Eq. (2) can be solved by the alternate direction method of multiplier (ADMM). More details about ADMM can be found in Dragomiretskiy and Zosso (2014). Here, ADMM is used to optimize each modal component and center frequency and search saddle points of the incremental Lagrange function as well. With a combination of the Parseval/Plancherel Fourier isometry under L^2 norm, the mode u_q is updated and the optimization of ω_q takes place in the spectral domain (Dragomiretskiy and Zosso 2014). The process of solving Eq. (2) using ADMM is shown in Eqs. (4)-(6).

$$\hat{u}_q^{n+1}(\omega) \leftarrow \frac{\hat{x}(\omega) - \sum_{i \neq q} \hat{u}_i(\omega) + \frac{\hat{\lambda}(\omega)}{2}}{1 + 2\alpha(\omega - \omega_q)^2} \tag{4}$$

$$\omega_q^{n+1} \leftarrow \frac{\int_0^\infty \omega \left| \hat{u}_q^{n+1}(\omega) \right|^2 \mathrm{d}\omega}{\int_0^\infty \left| \hat{u}_q^{n+1}(\omega) \right|^2 \mathrm{d}\omega} \tag{5}$$

$$\hat{\lambda}^{n+1}(\omega) \leftarrow \hat{\lambda}^n(\omega) + \gamma \left[\hat{x}(\omega) - \sum_q \hat{u}_q^{n+1}(\omega) \right] \tag{6}$$

where γ is the noise tolerance and it should satisfy the fidelity requirement of signal decomposition. $\hat{u}_q^{n+1}(\omega)$, $\hat{u}_i(\omega)$, $\hat{x}(\omega)$ and $\hat{\lambda}(\omega)$ represent $u_q^{n+1}(t)$, $u_i(t)$, $x(t)$ and $\lambda(t)$ in spectral domain, respectively.

In a word, VMD takes the advantage of ADMM to generate a finite number of modes/components and center frequencies during each transform. Its main steps are as follows.

(1) Initialize $\hat{u}_q^1$, ω_q^1, λ^1 and the maximum number of iteration N, $n \leftarrow 0$;
(2) Update $\hat{u}_q$ and ω_q through Eqs. (4) and (5);
(3) Update $\hat{\lambda}$ by a use of Eq. (6);
(4) ε is defined as the tolerance/threshold to judge convergence. Generally, the suggested value of ε is assumed to be 1×10^{-6}. If $\sum_q \left\| \hat{u}_q^{n+1} - \hat{u}_q^n \right\|_2^2 / \left\| \hat{u}_q^n \right\|_2^2 < \varepsilon$ is not satisfied and $n < N$, return to Step 2, otherwise the iteration is terminated and the final values of $\hat{u}_q$ and ω_q are obtained.

3. Generalized adaptive variational modal decomposition theory

Although VMD shows its superiority on multi-component signal decomposition, it encounters two main challenges. The foremost challenge to be issued is that the number of modal components is required to be predefined adaptively. In addition, VMD does not work well on separating non-stationary signals composed of closely spaced or overlapped modes. Both of them needs to be solved urgently. Therefore, the GAVMD method is proposed and its flowchart is plotted in Fig. 1.

The GAVMD method consists of two main parts, that is, the adaptive selection of Q through an index of mean frequency and the generalized VMD by introducing the algorithm of generalized demodulation. Compared with

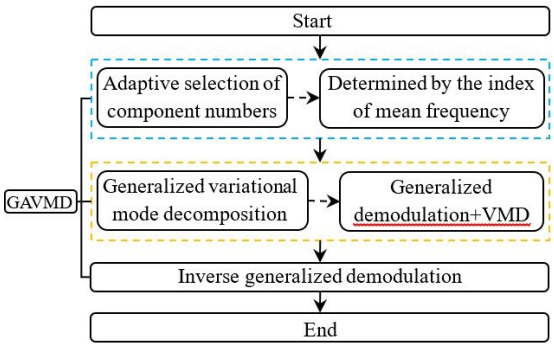

Fig. 1 The flowchart of the proposed GAVMD

classic VMD, GAVMD not only gets rid of the problem that the number of modal components cannot be determined adaptively, but also suppresses the mode overlapping problem among the extracted mono-components. Therefore, it is a promising decomposition method for non-stationary response signals.

3.1 Adaptive selection of component numbers

For a multi-component signal, pattern loss or sharing with neighboring modes is possible to happen if the signal is underbinning. In addition, the central frequencies of the decomposed components do not coincide with a premise of underbinning. By contrast, the important parts of the multi-component signal are shared by two or more different modes and their center frequencies coincide (mode duplication) when the signal is overbinning and the quadratic penalty factor of α is big (Dragomiretskiy and Zosso 2014). Otherwise, for a small α noises will be hidden in one or more extra modes and thus a broad spectral density is achieved. Based on this remarkable feature, an index of mean frequency is presented to adaptively define the number of modal components in advance.

In VMD, the target signal is decomposed into Q eigenmode functions in a frequency order from low to high. If the matrix consisting of Q eigenmode functions is flipped, the frequencies are then ranked from high to low orders. After that, Hilbert transform is performed on the VMD-processed matrix to estimate the IFs of components, followed by matrix flipping to obtain IFs from high to low orders. Subsequently, the mean frequency of each component (p_q) is calculated by averaging the elements of each vector of the obtained IFs. Finally, Q is determined by comparing the index of mean frequency with a threshold. The main iterative steps of this method are illustrated as follows.

(1) Normally, a multi-component signal is composed of two or more components. However, the number of components is unknown in advance. Therefore, VMD is used to separate the target signal into two components by setting $Q = 2$ at first, aiming to preventing that the decomposition of the target signal with two components is neglected. After that, the decomposed components constitute the matrix $\boldsymbol{u}$.

(2) The matrix $\boldsymbol{u}'$ is obtained by flipping $\boldsymbol{u}$.

(3) Hilbert transform is performed on each component (u_q) of $\boldsymbol{u}'$ and then their individual mean frequencies (p_q) are solved.

(4) Let $\sigma = p_q - p_{q\text{-}1}$. If $\sigma > -\theta$, the signal is assumed to be overbinning and the iteration is terminated. At this moment, the value of Q is solved and hence the number of components is defined as $Q - 1$. Otherwise, use $Q + 1$ instead of Q and then repeat Steps (1)~(3) until $\sigma > -\theta$ is satisfied.

Here, θ represents the threshold and its suggested range is 0.01~0.02. For multi-component signals with overlapped modes, 0.01 is recommended. It is noted that θ cannot be smaller than 0.005 because overbinning is likely to happen for a too small θ. Actually, if the phenomenon of overbinning happens, σ will be very small whatever it is positive or negative. As such, the overbinning is bound to happen if we select a minus threshold ($-\theta$) smaller than σ.

3.2 Generalized variational modal decomposition

To better understand the generalized demodulation variational modal decomposition, it is appropriate to introduce the generalized demodulation algorithm proposed by Olhede and Walden (2005) at first. The main goal of the generalized demodulation theorem is to deal with the problem of closely spaced or overlapped modes. To be specific, its essence is the generalized Fourier transform, which extends the frequency-shifted nature of the Fourier transform from constant cases to time-varying scenarios (Feng *et al.* 2020). By performing the generalized demodulation, the time-frequency distribution of the response signal is demodulated from a curve into a straight line parallel to the time axis. After that, the components are successfully extracted by a use of band-pass filters and inverse demodulation.

The whole schematic diagram of the generalized demodulation algorithm is illustrated in Fig. 2. As shown in Fig. 2, BW denotes the bandwidth of the target signal and it is exactly the differential between the highest and the lowest frequencies of the harmonics from the target signal. In contrast, BW_{AM} represents the bandwidth of the demodulated AM signal. With a comparison of BW and BW_{AM}, we can find that BW_{AM} is dramatically smaller than BW, which means the generalized demodulation algorithm is capable of converting broadband signals into narrowband signals. Thus, VMD gets rid of the restriction that it is only suitable for narrowband signals. The details of the

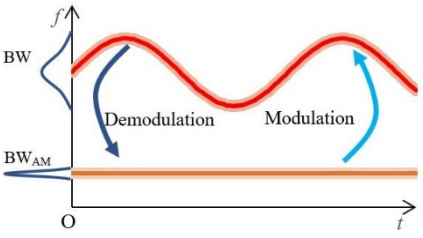

Fig. 2 The schematic diagram of the generalized demodulation

generalized demodulation are described as follows.

For a multi-component signal as shown in Eq. (1), its analytical signal is established by the Hilbert transform and expressed by Eq. (7).

$$x_A(t) = x(t) + \mathrm{jH}[x(t)] \tag{7}$$

where $\mathrm{H}[\cdot]$ represents the Hilbert transform of the function inside the square bracket.

As shown in Eq. (8), the analytic signal $x_A(t)$ is then demodulated in a generalized manner.

$$x_A^d(t) = \int_{-\infty}^{+\infty} x_A(t)\Phi^-(t)\mathrm{d}t \tag{8}$$

in which $\Phi^-(t)$ is a demodulation operator (DO) and its expression is illustrated in Eq. (9).

$$\Phi^-(t) = e^{-j2\pi\int[\hat{f}(t)-f_0]\mathrm{d}t} = e^{-js_0(t)} \tag{9}$$

where $\hat{f}(t)$ is the estimated IF of each component and it can be pre-estimated by TFA methods such as SWT. f_0 represents the carrier frequency and the value of $\hat{f}(t)$ at the initial moment is usually set as f_0 by default. $s_0(t)$ denotes the real phase function that varies with time and its expression is $s_0(t) = 2\pi\int[\hat{f}(t) - f_0]\mathrm{d}t$. Actually, f_0 does not need to be defined precisely because its value has little effect on the signal decomposition results.

Conversely, the analytic signal can be obtained by performing the modulation operator (MO) on the demodulated signal, which is expressed as Eq. (10). Since $\Phi^-(t)\cdot\Phi^+(t) = 1$ can be achieved according to Eqs. (9) and (11), MO is actually regarded as an inverse operation of DO.

$$x_A(t) = \int_{-\infty}^{+\infty} x_A^d(t)\Phi^+(t)\mathrm{d}x \tag{10}$$

where $\Phi^+(t)$ is the modulation operator (MO) as expressed in Eq. (11).

$$\Phi^+(t) = e^{j2\pi\int[\hat{f}(t)-f_0]\mathrm{d}t} \tag{11}$$

Following the introduction of the generalized demodulation theorem, the specific steps of the generalized variational modal decomposition are detailed as follows.

(1) The Hilbert transform of the target signal $x(t)$ yields the analytic signal $x_A(t)$.
(2) An appropriate conversion factor $s_0(t)$ is predefined and $x_A(t)$ is then processed by the generalized demodulation algorithm to obtain the demodulated signal $x_A^d(t)$.
(3) By performing VMD on the real part of the $x_A^d(t)$, a total of Q components (u_q') is obtained. Here, Q is adaptively defined by the method in Section 3.1. After that, Hilbert transform is applied to the obtained u_q' to establish the analytic signals of each component (u_{qA}').
(4) The inverse generalized demodulation transform (also called MO) is applied on u_{qA}' to get the analytical signal (u_{qA}) of the component signal (u_q) which originates from the target signal $x(t)$. Then, u_q can be extracted by taking the real part of u_{qA}. Thereby, the decomposition is finally finished.

4. Numerical examples

4.1 A multi-component signal with two mode overlapped FM components

To verify the effectiveness of the above mentioned method, a multi-component signal with two mode overlapped FM components as shown in Eq. (12) is considered.

$$\begin{aligned} x(t) &= x_1(t) + x_2(t) \\ &= \cos[2\pi(0.55t^2 + 7t)] + \cos[2\pi(t^2 + 7.5t)] \end{aligned} \tag{12}$$

The theoretic IFs of $x_1(t)$ and $x_2(t)$ are $f_1(t) = 1.1\,t + 7\,\mathrm{Hz}$ and $f_2(t) = 2\,t + 7.5\,\mathrm{Hz}$, respectively. The sampling frequency is 200 Hz and the sampling time is 10 seconds. The time domain waveform and Fourier spectrum of $x(t)$ are plotted in Figs. 3(a) and (b), respectively. As seen in Fig. 3(b), there are no obvious peaks in the spectrum, which implies that the components of $x(t)$ are overlapped in frequency domain. According to the IF expressions of $x_1(t)$ and $x_2(t)$, $f_1(t)$ varies from 7 to 18 Hz, while $f_2(t)$ changes in the range between 7.5 and 27.5 Hz during the time period from t = 0 to t = 10 sec. That is to say, $f_1(t)$ and $f_2(t)$ overlap within the frequency band from 7.5 to 18 Hz, which gives a good interpretation of the mixed/overlapped modes in Fourier spectrum. Thus, the proposed GAVMD method is utilized to extract each component signal from the target signal $x(t)$.

At first, Q = 2 are preset and then VMD is used to decompose $x(t)$. Subsequently, the mean frequency of each component signal is solved and the result is plotted in Fig. 4(a). As seen in Fig. 4(a), $\sigma = p_q - p_{q-1} = p_2 - p_1 <$ -0.01 when Q = 2. It implies that the precondition of $\sigma >$ -θ is not satisfied. Therefore, the procedure mentioned above is repeated by setting Q = 3 and the corresponding result is

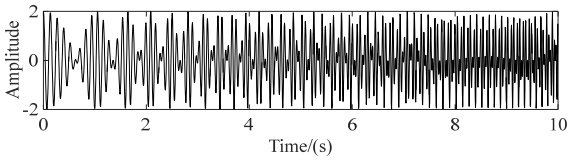

(a) Waveform

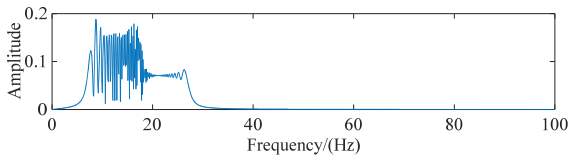

(b) Spectrum

Fig. 3 The time domain waveform and Fourier spectrum of $x(t)$

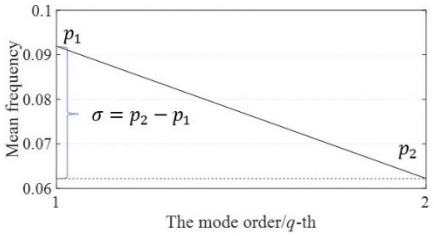

(a) $Q = 2$

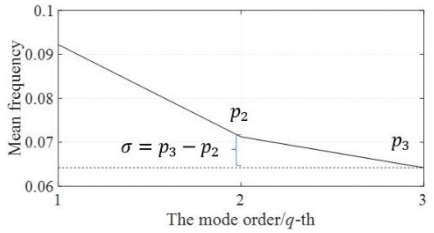

(b) $Q = 3$

Fig. 4 Mean frequency with various Q

plotted in Fig. 4(b). It can be seen from Fig. 4(b) that $\sigma = p_q - p_{q-1} = p_3 - p_2 >$ -0.01 when Q = 3. That is to say, overbinning occurs if Q = 3. Therefore, Q = 2 is selected as the number of components in $x(t)$. It is noted here that the calculation of σ and its comparison with the threshold can be carried out adaptively on condition that VMD is performed.

Then, Hilbert transform is performed on the target signal $x(t)$ to yield the analytic signal $x_A(t)$. After that, the initial value of $\hat{f}(t)$, estimated by SWT, is chosen as f_0 and thus an appropriate conversion factor $s_0(t)$ is established. With a proper selection of $s_0(t)$, $x_A(t)$ is demodulated to get $x_A^d(t)$ according to Eq. (8) and then VMD is applied on the real part of the $x_A^d(t)$ to obtain two individual components (u_q'). By performing Hilbert transform on the u_q', the analytic signal u_{qA}' is established and then the inverse generalized demodulation is applied on them to gain u_{qA}. Finally, u_q is extracted by taking the real part of u_{qA} and the results are illustrated in Fig. 5.

It can be clearly seen from Fig. 5 that the component signals decomposed by the GAVMD agrees well with their theoretical counterparts. Comparatively, the component signals decomposed by the standard VMD is not in good accordance with that of theoretical counterparts. Therefore, a conclusion can be drawn that the GAVMD behaves better than the standard VMD on the decomposition of multi-component signals with overlapped modes. The IFs of the decomposed mono-components are extracted by performing SWT and the results are shown in Fig. 6. As illustrated in Fig. 6, the IFs identified by GAVMD+SWT are in good agreement with their theoretical counterparts. Compared with VMD + SWT, the proposed GAVMD + SWT method is capable of extracting the IF of each component with higher accuracy during the period from about t = 0 to t = 1 sec. Thus, the superiority of the proposed GAVMD + SWT is demonstrated.

4.2 A multi-component signal with three mode overlapped AM-FM components

In Section 4.1, only FM signal is investigated, however, the amplitude may pose a significant impact on signal decomposition. Therefore, a multi-component signal with three mode overlapped AM-FM components as indicated in Eq. (13) is considered.

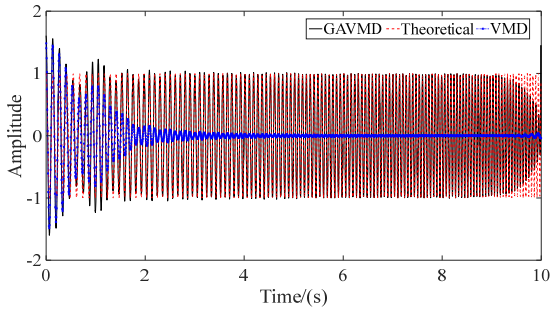

(a) $x_1(t)$

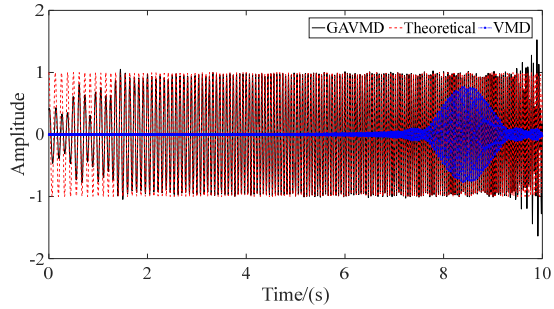

(b) $x_2(t)$

Fig. 5 The components decomposed by GAVMD and VMD

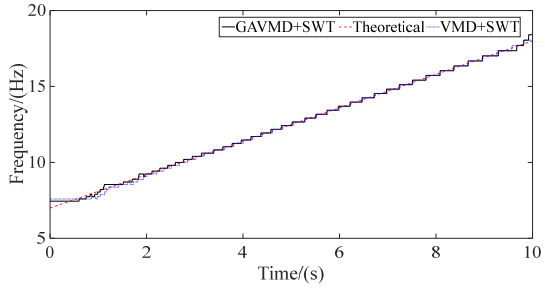

(a) $x_1(t)$

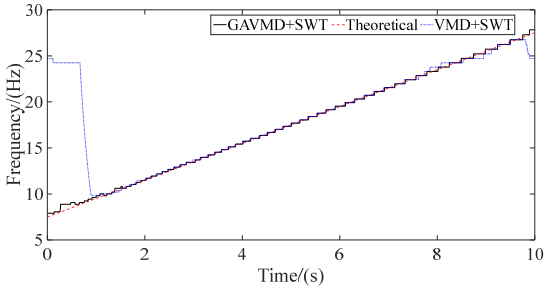

(b) $x_2(t)$

Fig. 6 The IFs extracted by GAVMD + SWT and VMD + SWT

$$\begin{aligned} y(t) &= y_1(t) + y_2(t) + y_3(t) \\ &= 12\mathrm{e}^{-0.05t}\cos[2\pi(0.1t^3 - 0.3t^2 + 6t)] \\ &\quad +10\mathrm{e}^{-0.1t}\cos[2\pi(0.3t^3 - 0.5t^2 + 7t)] \\ &\quad +13\mathrm{e}^{-0.1t}\cos[2\pi(0.5t^3 - 0.8t^2 + 8.1t)] \end{aligned} \tag{13}$$

The theoretical frequencies of the three components are $f_1 = 0.3\,t^2 - 0.6\,t + 6$ Hz, $f_2 = 0.9\,t^2 - t + 7$ Hz and $f_3 = 1.5\,t^2 - 1.6\,t + 8.1$ Hz, respectively. In this case, a sampling rate of 500 Hz is used and the total sampling time is set to be 10 seconds. To consider the influence of the

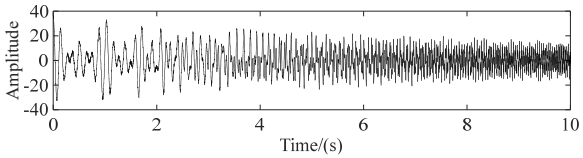

(a) Waveform

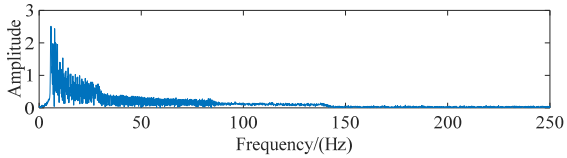

(b) Spectrum

Fig. 7 The time domain waveform and Fourier spectrum of the noisy $y(t)$

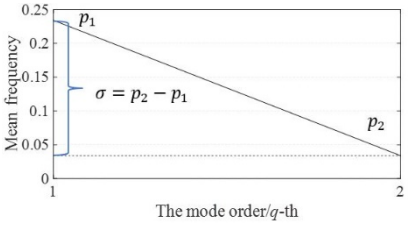

(a) $Q = 2$

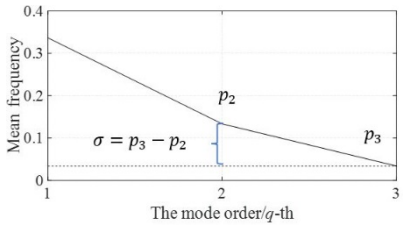

(b) $Q = 3$

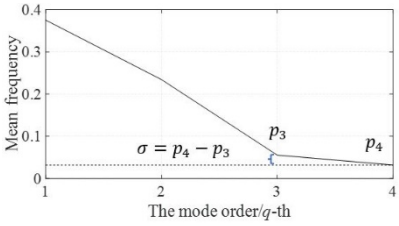

(c) $Q = 4$

Fig. 8 Mean frequency with various Q

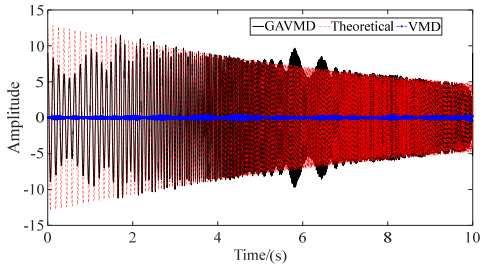

(a) $y_1(t)$

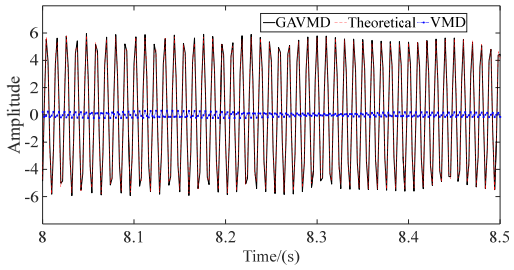

(b) $y_1(t)$ during the period from $t = 8$ to $t = 8.5$ sec

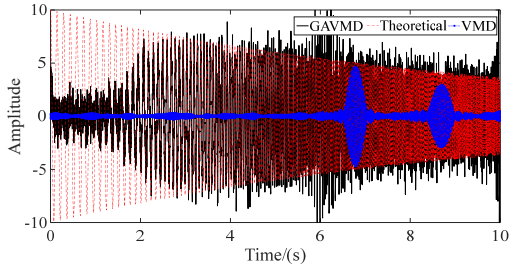

(c) $y_2(t)$

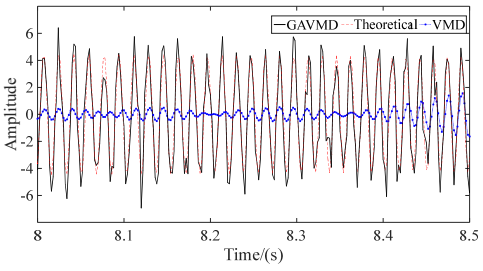

(d) $y_2(t)$ during the period from $t = 8$ to $t = 8.5$ sec

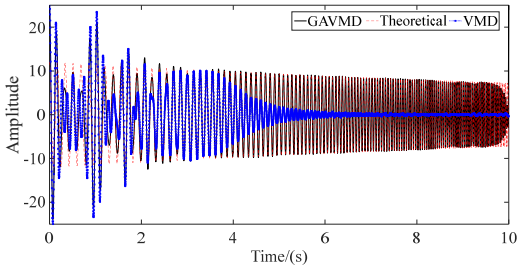

(e) $y_3(t)$

Fig. 9 The components decomposed by GAVMD and VMD

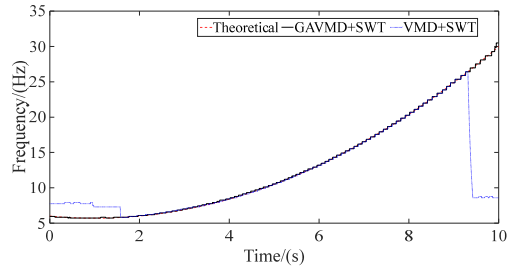

(a) $y_1(t)$

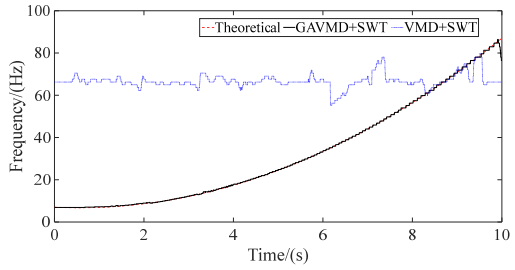

(b) $y_2(t)$

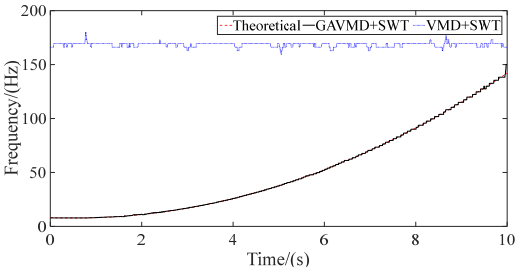

(c) $y_3(t)$

Fig. 10 The IFs extracted by GAVMD + SWT and VMD + SWT

noise, a simulated 10% Gaussian white noise is added to the target signal. The noise intensity is defined by signal-to-noise ratio (SNR) expressed in Eq. (14). As shown in Eq. (14), SNR is closely linked with the percentage of noise level. For example, SNR = 20 dB will be acquired if we substitute e = 10 into Eq. (14). Here, e = 10 implies 10% Gaussian white noise is considered.

$$\begin{aligned}\mathrm{SNR} &= 10\lg\left(\frac{P_{\mathrm{Signal}}}{P_{\mathrm{Noise}}}\right) = 10\lg\left(\frac{A^2_{\mathrm{Signal}}}{A^2_{\mathrm{Noise}}}\right) \\ &= 20\lg\left(\frac{A_{\mathrm{Signal}}}{A_{\mathrm{Noise}}}\right) = 20\lg\left(\frac{100}{e}\right)\end{aligned} \tag{14}$$

where P_{Signal} and P_{Noise} represent the average powers of the original signal and the noisy signal, respectively. A_{Signal} and A_{Noise} separately denote the amplitudes of the original signal and the noisy signal. e is the percentage of noise level, which also refers to the ratio between A_{Noise} and A_{Signal}.

The target signal contaminated by 10% Gaussian white noise is plotted in Fig. 7(a), while its Fourier spectrum is displayed in Fig. 7(b). As shown in Fig. 7(b), none of apparent peaks appears in the spectrum, which indicates the modes of $y(t)$ are overlapped in frequency domain.

Similar to the previous numerical case in Section 4.1, the index of mean frequency is used to select the number of

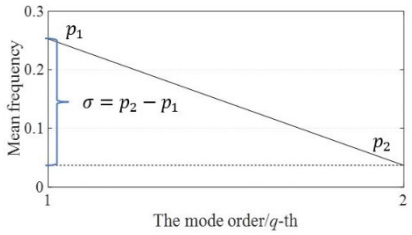

(a) Q = 2

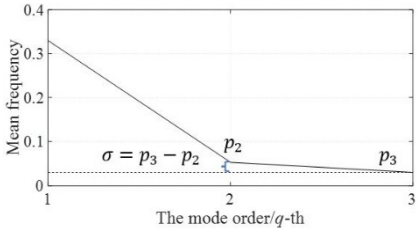

(b) Q = 3

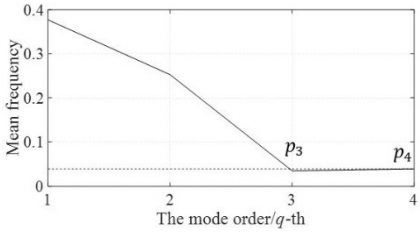

(c) Q = 4

Fig. 11 Mean frequency with various Q under 20% Gaussian white noise

modal components and the results are shown in Fig. 8. As shown in Fig. 8, $\sigma = p_4 - p_3 >$ -0.01 when Q equals 4. Thus, the number of components in $y(t)$ is set as 3.

After that, the generalized VMD algorithm is performed on the noisy $y(t)$ and the results are plotted in Fig. 9. As shown in Fig. 9, the components decomposed by the proposed GAVMD agree with the theoretical counterparts better than that of VMD. To extract the IFs of the decomposed mono-components, SWT is performed and the resultant IF curves are illustrated in Fig. 10. It can be seen from Fig. 10 that VMD recognizes the Gaussian white noise as a component signal. Thus, VMD + SWT can only extract the IFs of $y_1(t)$ effectively, but does not behave well on the IF extraction of $y_2(t)$ and $y_3(t)$. By contrast, the GAVMD+SWT method is able to extract the IFs of each component more accurately than VMD + SWT, even though the target signal $y(t)$ is contaminated by 10% Gaussian white noise.

Similarly, 20% and 30% Gaussian white noises are considered. The results of the mean frequencies under different noises are shown in Figs. 11 and 12, respectively. As seen in Figs. 11 and 12, the signals contaminated by 20% and 30% Gaussian white noises are overbinning when Q = 4 since $\sigma = p_4 - p_3 > -0.01$. Therefore, the number of components in the noisy $y(t)$ with 20% and 30% Gaussian white noises is set as 3.

After that, GAVMD+SWT and VMD+SWT are used to process the noisy signals mentioned above and the resultant IF curves are shown in Figs. 13 and 14. As illustrated in

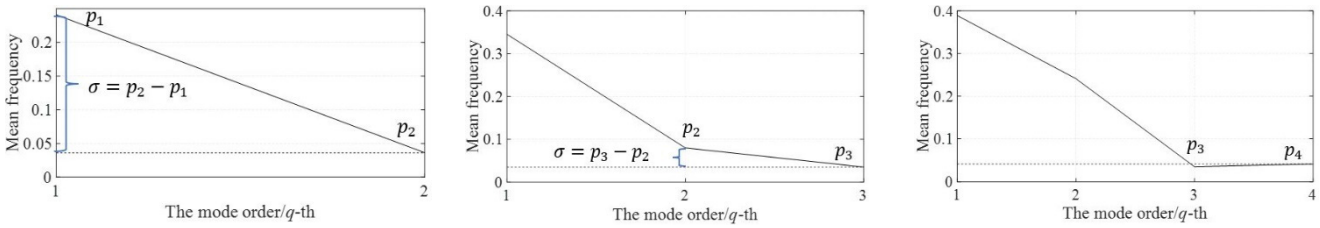

(a) $Q = 2$ (b) $Q = 3$ (c) $Q = 4$

Fig. 12 Mean frequency with various Q under 30% Gaussian white noise

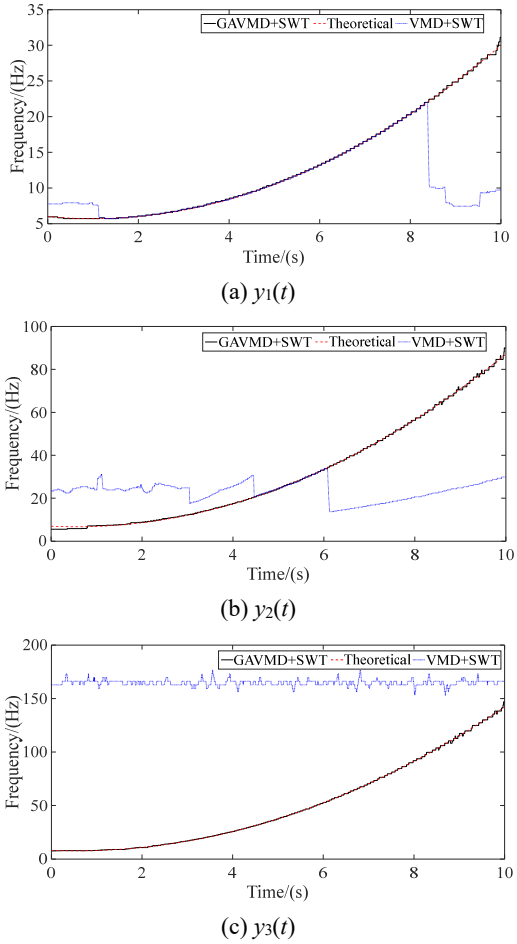

(a) $y_1(t)$ (b) $y_2(t)$ (c) $y_3(t)$

Fig. 13 The IFs extracted from $y(t)$ with 20% Gaussian white noise

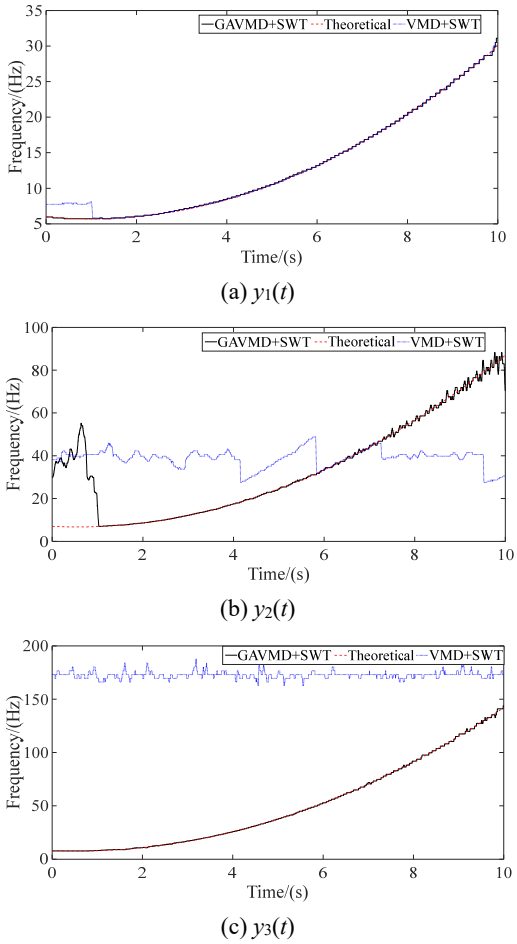

(a) $y_1(t)$ (b) $y_2(t)$ (c) $y_3(t)$

Fig. 14 The IFs extracted from $y(t)$ with 30% Gaussian white noise

Figs. 13 and 14, VMD+SWT can only extract the IF of $y_1(t)$ effectively. Compared with VMD + SWT, GAVMD + SWT is able to extracting the IFs of $y_1(t)$, $y_2(t)$ and $y_3(t)$ accurately. Although Gaussian white noises possess an impact on IF identification, the proposed GAVMD+SWT method can still extract the IF curves of components from noisy $y(t)$ effectively, which demonstrate its good robustness on noise resistance.

4.3 A mass-spring-damper model

To verify the effectiveness and accuracy of the proposed method, a typical mass-spring-damper model having three degree of freedoms is simulated and shown in Fig. 15. The properties of mass, stiffness and damping are provided in Eq. (15).

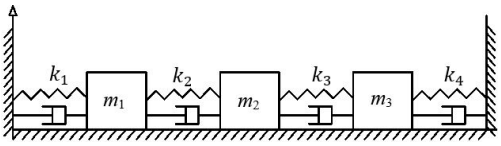

Fig. 15 The mass-spring-damper model

$$\begin{cases} m_1 = m_2 = m_3 = 12 \text{ kg} \\ k_1 = k_4 = 1500 + 3000t \text{ N/m} \\ k_2 = k_3 = 1000 + 3000t \text{ N/m} \\ c = 3\text{N} \cdot \text{s/m} \end{cases} \tag{15}$$

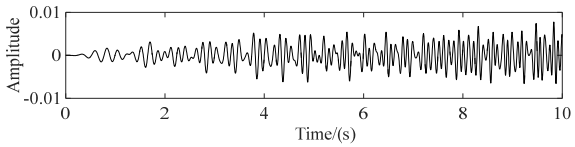

(a) Waveform

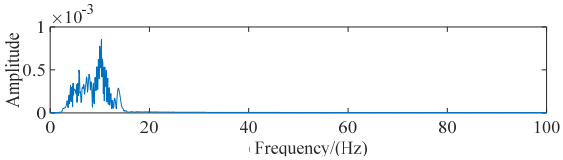

(b) Spectrum

Fig. 16 The time domain waveform and Fourier spectrum of the mass-spring-damper model

where m, k, and c represents mass, stiffness and damping, respectively.

In Eq. (15), the total sampling time is set as 10 seconds. Assuming that the model is subjected to stochastic excitation of Gaussian white noise with zero mean, the viscous damper is investigated alone in this numerical example, without an extra consideration of frictional damping and other energy consumption.

Generally, the vibration differential equation of the N-degree-of-freedom structural system is expressed as Eq. (16) (Ferhatoglu *et al*. 2018).

$$\boldsymbol{M}\ddot{\boldsymbol{x}} + \boldsymbol{C}\dot{\boldsymbol{x}} + \boldsymbol{K}\boldsymbol{x} + \boldsymbol{F}_{non} = \boldsymbol{F} \tag{16}$$

where $\boldsymbol{F}_{non}$ is the local nonlinear internal force vector; $\boldsymbol{F} = [\boldsymbol{F}_1, \ldots, \boldsymbol{F}_N]^T$ is the external force vector applied on the system; $\boldsymbol{M}$, $\boldsymbol{C}$, $\boldsymbol{K}$ represent the N dimensional mass, damping and stiffness matrix, respectively; $\boldsymbol{x} = (x_1, \ldots, x_N)^T$ denotes the displacement response vector of the system; $\dot{\boldsymbol{x}}$ and $\ddot{\boldsymbol{x}}$ separately represent the first order and second order derivatives of $\boldsymbol{x}$, namely the velocity and acceleration response vector. When $\boldsymbol{F}_{non}$ is zero, Eq. (16) will turn into Eq. (17), which is exactly the basic structural system used for describing the mass-spring-damper model in this section.

$$\boldsymbol{M}\ddot{\boldsymbol{x}} + \boldsymbol{C}\dot{\boldsymbol{x}} + \boldsymbol{K}\boldsymbol{x} = \boldsymbol{F} \tag{17}$$

The Runge-Kutta method is employed to solve Eq. (17) and the resultant acceleration responses of $\ddot{x}_1$, $\ddot{x}_2$ and $\ddot{x}_3$ can be achieved without difficulty. All these three acceleration responses are suitable for signal decomposition and IF extraction. Here, $\ddot{x}_3$ is set for example and its time-domain waveform and Fourier spectrum are shown in Figs. 16(a) and (b), respectively. It can be seen from Fig. 16(b) that the modes of the acceleration response are overlapped due to there are no obvious peaks. The index of mean frequency is utilized to determine the number of modal components and the results are shown in Fig. 17. As illustrated in Fig. 17(c), $\sigma = p_2 - p_1 > -0.01$ when Q = 4, which implies the phenomenon of overbinning has occurred. As such, the number of modes or components is defined as 3.

Similarly, the carrier frequency f_0 as well as $s_0(t)$ is selected to perform the generalized variational modal

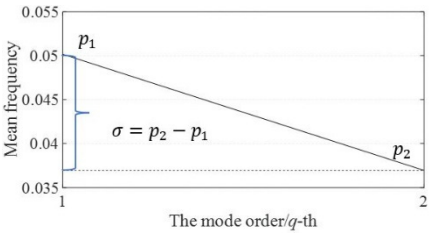

(a) Q = 2

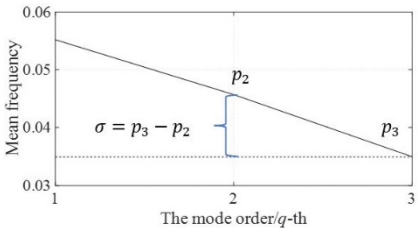

(b) Q = 3

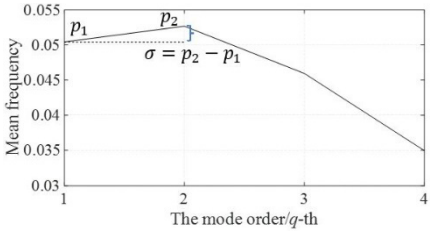

(c) Q = 4

Fig. 17 Mean frequency with various Q

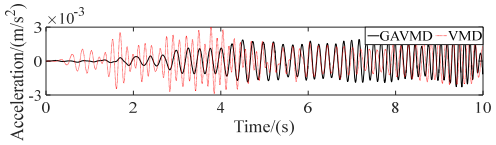

(a) IMF1

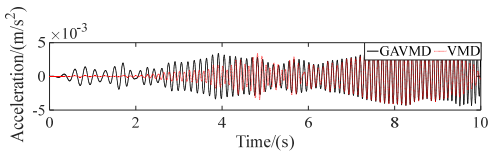

(b) IMF2

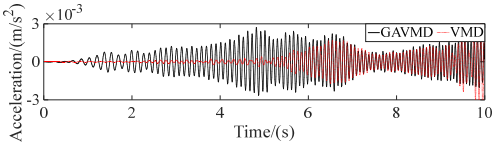

(c) IMF3

Fig. 18 The time domain waveform of the decomposed component signals

decomposition, and the resultant components are presented in Fig. 18. Since there are no theoretical components for comparison, SWT is performed for the IF extraction and the results are plotted in Fig. 19. The theoretical IFs of each mode are obtained by solving the eigenvalues of Eq. (17) and then presented in Fig. 19.

It can be clearly seen from Fig. 19 that the proposed

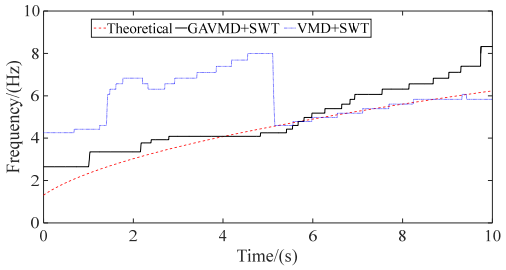

(a) IMF1

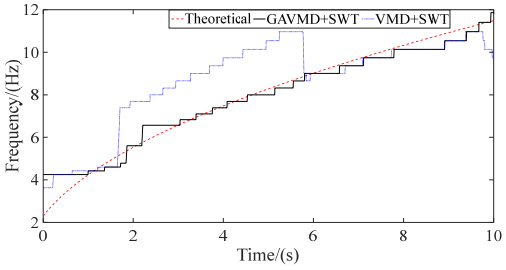

(b) IMF2

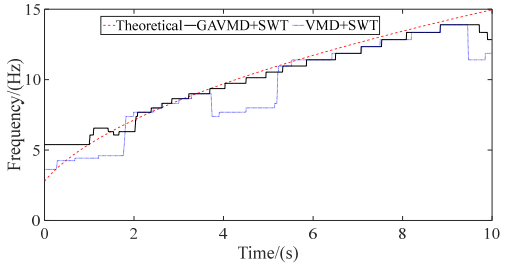

(c) IMF3

Fig. 19 The IFs extracted by GAVMD + SWT and VMD + SWT

GAVMD + SWT can extract the IFs of each component signal effectively and its identified IFs agree with the theoretical counterparts well. By contrast, the IFs identified by the VMD + SWT still exhibit the features of closely spaced and overlapped modes, which reveals that VMD cannot separate the mode overlapped components well. Therefore, a conclusion can be drawn that GAVMD behaves better than VMD on overlapped modes decomposition.

5. Experimental case study

To further validate the accuracy of the GAVMD for nonstationary signals with closely-spaced components, a cable composed of pieces of 7Φ5 steel wires is considered (Wang *et al*. 2013, Liu *et al*. 2019). The cable has elastic modulus E = 1.95 × 10^5 MPa, area of cross section A = 1.374 × 10^4 m^2, density of unit length ρ = 1.1 kg/m. The total length of the cable between two ends is 4.55 m. The accelerometer is installed vertically at the mid-point of the cable. The time-varying tension force is applied on the cable through a MTS loading systems so that the stiffness of the cable changes with time, which also results in the time-dependent natural frequency of the cable. The test setup is shown in Fig. 20.

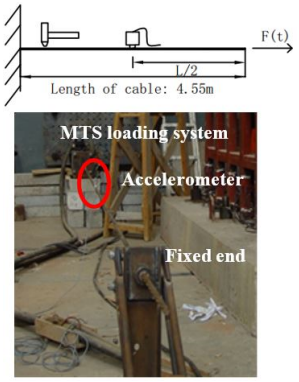

Fig. 20 The cable test setup

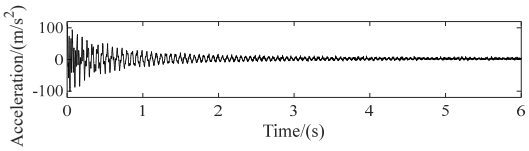

(a) The measured

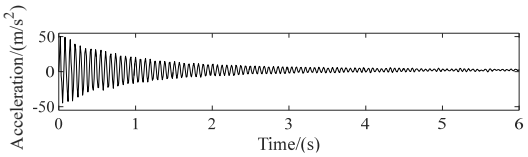

(b) The processed

Fig. 21 Acceleration response signals

During the testing, the initial tension force of the cable was set to 20 kN, and then the tension force increased linearly at the rate of 1.67 kN/s using the MTS load system. At the same time, the impact hammer was used to generate free vibration and the vertical acceleration response was recorded with a sampling frequency of 600 Hz. The duration of data acquisition was set to be 6 sec.

The measured acceleration response signal is shown in Fig. 21(a). To reduce the ambient noise, a Butterworth low-pass filter (30 Hz) and an operation of resampling with 100 Hz are performed on the measured signal and the processed acceleration response signal is plotted in Fig. 21(b). It should be noted here that closely-spaced modes are not considered in this test. To address this issue, a frequency-modulated signal whose frequency is close to the counterpart of the steel cable is simulated and shown as Eq. (18). Subsequently, the simulated signal and the processed acceleration response signal of the cable are mixed and the result is shown in Fig. 22(a). Fig. 22(b) also gives a visualization of the Fourier spectrum of the mixed signal. As seen in Fig. 22(b), there are no obvious peaks in the spectrum, which indicates the components of the mixed signal are overlapped in frequency domain.

$$z(t) = 45\cos\left[2\pi(0.32t^2 + 12.7t)\right] \tag{18}$$

The index of mean frequency is used to determine the number of modes of the mixed signal and the results are shown in Fig. 23. It is shown in Fig. 23 that $\sigma = p_3 - p_2$

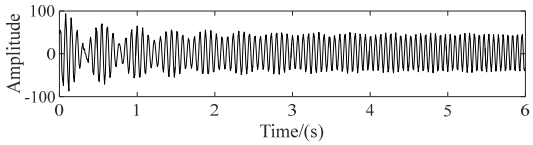

(a) The time domain waveform

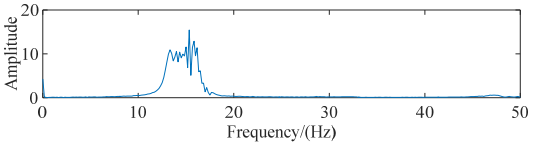

(b) Fourier spectrum

Fig. 22 The mixed signal and its Fourier spectrum

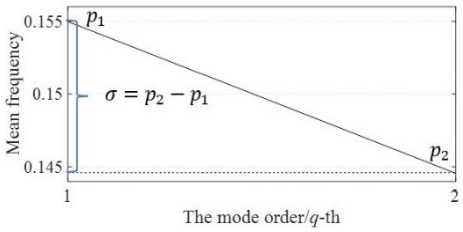

(a) $Q = 2$

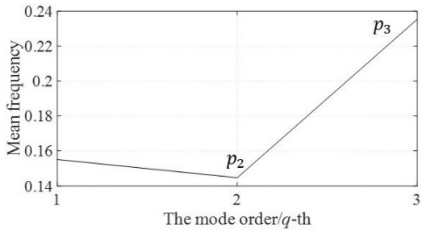

(b) $Q = 3$

Fig. 23 Mean frequency of the mixed signal with various Q

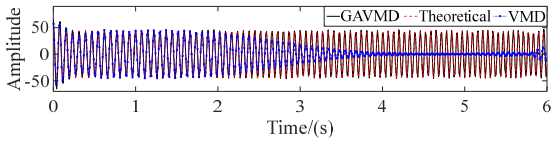

(a) $z(t)$

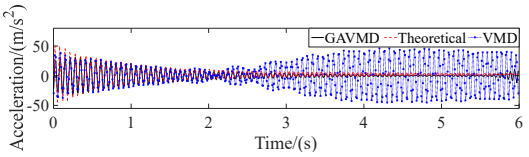

(b) the 1st order mode

Fig. 24 The components decomposed by GAVMD and VMD

> -0.01 when the number of modes or components (Q) is 3. That is to say, the phenomenon of overbinning occurs if Q equals 3. Therefore, the number of components is determined as 2. After that, VMD and GAVMD are separately performed on the mixed signal and the results are plotted in Fig. 24. As shown in Fig. 24, GAVMD behaves much better than VMD on the decomposition of mode

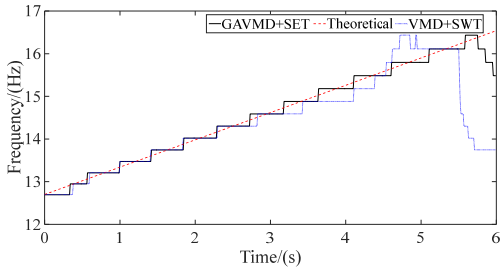

(a) $z(t)$

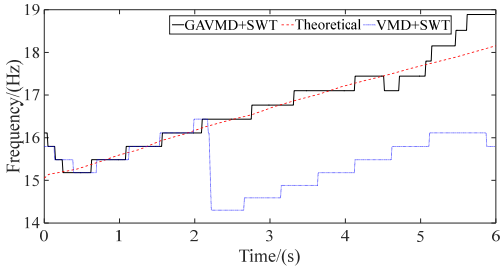

(b) the 1st order mode

Fig. 25 The IFs extracted by GAVMD + SWT and VMD + SWT

closely-spaced signals, which verifies its superiority once again. Following the process of signal decomposition, SWT is performed on the decomposed components and the IF extraction results are plotted in Fig. 25. Here, only the fundamental frequencies of the cable at several fixed tension forces are considered for simplicity, which is then used as theoretical IFs to compare with the extracted IFs of the 1st order mode. It can be seen from Fig. 25 that GAVMD + SWT is able to extracting IFs effectively, but VMD + SWT does not work well.

6. Conclusions

As a newly developed technique, VMD cannot adaptively decompose a non-stationary signal composed of overlapped modes. Therefore, GAVMD is developed to address this issue. The proposed GAVMD method can be divided into two parts, namely adaptive selection of Q using the index of mean frequency and the generalized VMD by introducing the generalized demodulation algorithm. Compared with classic VMD, GAVMD not only gets rid of the problem that the number of modal components is not determined adaptively, but also overcomes the drawback of mode overlapping among the extracted mono-components. After that, SWT is utilized to extract IFs of the decomposed components to better understand the proposed GAVMD. Three numerical examples and a steel cable with time-varying tension force are investigated to verify the validity and accuracy of the proposed method. The results demonstrate that the proposed GAVMD method is capable of decomposing a multi-component signal with overlapped modes into several mono-components effectively and its combination with SWT enables a successful IF extraction of each individual component as well. However, our research is to present a general approach for the decomposition of

nonstationary signals with several closely spaced or overlapped mono-components. Future work will be dedicated to its application on response signals of real structures.

Acknowledgments

This study is sponsored by the National Natural Science Foundation of China (NSFC) under Grants No. 51608122, China Postdoctoral Science Foundation under Grants No. 2018M632561, the Natural Science Foundation of the Fujian Province under Grants No. 2020J01581 and the Special fund for science and technology innovation of Fujian Agriculture and Forestry University under Grants No. CXZX2020112A.

References

Auger, F. and Flandrin, P. (1995), "Improving the readability of time-frequency and time-scale representations by the reassignment method", *IEEE Trans. Sig. Pr.*, **43**(5), 1068-1089. https://doi.org/10.1109/78.382394

Bagheri, A., Ozbulut, O.E. and Harris, D.K. (2018), "Structural system identification based on variational mode decomposition", *J. Sound Vib.*, **417**, 182-197. https://doi.org/10.1016/j.jsv.2017.12.014

Cempel, C. and Tabaszewski, M. (2007), "Multidimensional condition monitoring of machines in non-stationary operation", *Mech. Syst. Sig. Pr.*, **21**(3), 1233-1241. https://doi.org/10.1016/j.ymssp.2006.04.001

Chen, X.Y. and Cui, B.B. (2016), "Efficient modeling of fiber optic gyroscope drift using improved EEMD and extreme learning machine", *Signal Process.*, **128**, 1-7. https://doi.org/10.1016/j.sigpro.2016.03.016

Chen, G.D. and Wang, Z.C. (2012), "A signal decomposition theorem with Hilbert transform and its application to narrowband time series with closely-spaced frequency components", *Mech. Syst. Sig. Pr.*, **28**, 258-279. https://doi.org/10.1016/j.ymssp.2011.02.002

Chen, S.Q., Yang, Y., Dong, X.J., Xing, G.P., Peng, Z.K. and Zhang, W.M. (2019), "Warped variational mode decomposition with application to vibration signals of varying-speed rotating machineries", *IEEE Trans. Instrum. Meas.*, **68**(8), 2755-2767. https://doi.org/10.1109/TIM.2018.2869440

Clausel, M., Oberlin, T. and Perrier, V. (2015), "The monogenic synchrosqueezed wavelet transform: A tool for the decomposition/demodulation of AM-FM images", *Appl. Comput. Harmon. Anal.*, **39**(3), 450-486. https://doi.org/10.1016/j.acha.2014.10.003

Daubechies, I., Lu, J.F. and Wu, H.T. (2011), "Synchrosqueezed wavelet transforms: an empirical mode decomposition-like tool", *Appl. Comput. Harmon. Anal.*, **30**(2), 243-261. https://doi.org/10.1016/j.acha.2010.08.002

Dragomiretskiy, K. and Zosso, D. (2014), "Variational mode decomposition", *IEEE Trans. Sig. Pr.*, **62**(3), 531-544. https://doi.org/10.1109/TSP.2013.2288675

Feldman, M. (2006), "Time-varying vibration decomposition and analysis based on the Hilbert transform", *J. Sound Vib.*, **295**(3-5), 518-530. https://doi.org/10.1016/j.jsv.2005.12.058

Feng, Z.P., Yu, X.N., Zhang, D. and Liang, M. (2020), "Generalized adaptive mode decomposition for nonstationary signal analysis of rotating machinery: Principle and applications", *Mech. Syst. Sig. Pr.*, **136**, 106530. https://doi.org/10.1016/j.ymssp.2019.106530

Ferhatoglu, E., Cigeroglu, E. and Özgüven, H.N. (2018), "A new modal superposition method for nonlinear vibration analysis of structures using hybrid mode shapes", *Mech. Syst. Sig. Pr.*, **107**, 317-342. https://doi.org/10.1016/j.ymssp.2018.01.036

Mohanty, Gupta, K.K. and Raju, K.S. (2014), "Bearing fault analysis using variational mode decomposition", *Proceedings of the 9th International Conference on Industrial and Information Systems*, Gwalior, India, December, pp. 1-6. https://doi.org/10.1109/ICIINFS.2014.7036617

Huang, N.E., Shen, Z., Long, S.R., Wu, M.C., Shih, H.H., Zheng, Q., Yen, N.C., Tung, C.C. and Liu, H.H. (1998), "The empirical mode decomposition and the Hilbert spectrum for nonlinear and non-stationary time series analysis", *Proc. Math. Phys. Eng. Sci.*, **454**, 903-995. https://doi.org/10.1098/rspa.1998.0193

Isham, M.F., Leong, M.S., Lim, M.H. and Ahmad, Z.A. (2018), "Variational mode decomposition: mode determination method for rotating machinery diagnosis", *J. Vib.*, **20**(7), 2604-2621. https://doi.org/10.21595/jve.2018.19479

Lahmiri, S. (2014), "Comparative study of ECG signal denoising by wavelet thresholding in empirical and variational mode decomposition domains", *Healthc. Technol. Lett.*, **1**, 104-109. https://doi.org/10.1049/htl.2014.0073

Le, T.H. and Caracoglia, L. (2015), "High-order, closely-spaced modal parameter estimation using wavelet analysis", *Struct. Eng. Mech., Int. J.*, **56**(3), 423-442. https://doi.org/10.12989/sem.2015.56.3.423

Lee, J.H., Kim, J. and Kim, H.J. (2001), "Development of enhanced wigner-ville distribution function", *Mech. Syst. Sig. Pr.*, **15**(2), 367-398. https://doi.org/10.1006/mssp.2000.1365

Li, C. and Liang, M. (2012), "A generalized synchrosqueezing transform for enhancing signal time-frequency representation", *Signal Process.*, **92**(9), 2264-2274. https://doi.org/10.1016/j.sigpro.2012.02.019

Liu, J.L., Wang, Z.C., Ren, W.X. and Li, X.X. (2015), "Structural time-varying damage detection using synchrosqueezing wavelet transform", *Smart Struct. Syst., Int. J.*, **15**(1), 119-133. https://doi.org/10.12989/sss.2015.15.1.119

Liu, J.L., Wei, X.J., Qiu, R.H., Zheng, J.Y., Zhu, Y.J. and Laory, I. (2018), "Instantaneous frequency extraction in time-varying structures using a maximum gradient method", *Smart Struct. Syst., Int. J..*, **22**(3), 359-368. https://doi.org/10.12989/sss.2018.22.3.359

Liu, J.L., Zheng, J.Y., Wei, X.J., Ren, W.X. and Laory, I. (2019), "A combined method for instantaneous frequency identification in low frequency structures", *Eng. Struct.*, **194**, 370-383. https://doi.org/10.1016/j.engstruct.2019.05.057

Oberlin, T., Meignen, S. and Perrier, V. (2015), "Second-order synchrosqueezing transform or invertible reassignment? Towards ideal time-frequency representations", *IEEE Trans. Sig. Pr.*, **63**(5), 1335-1344. https://doi.org/10.1109/TSP.2015.2391077

Olhede, S. and Walden, A.T. (2005), "A generalized demodulation approach to time-frequency projections for multicomponent signals", *Proc. R. Soc. A.*, **461**(2059), 2159-2179. https://doi.org/10.1098/rspa.2005.1455

Poon, C.W. and Chang, C.C. (2007), "Identification of nonlinear elastic structures using empirical mode decomposition and nonlinear normal modes", *Smart Struct. Syst.*, **3**(4), 423-437. https://doi.org/10.12989/sss.2007.3.4.423

Smith, J.S. (2005), "The local mean decomposition and its application to EEG perception data", *J. R. Soc. Interface*, **2**, 443-454. https://doi.org/10.1098/rsif.2005.0058

Thakur, G., Brevdo, E., Fučkar, N.S. and Wu, H.T. (2013), "The Synchrosqueezing algorithm for time-varying spectral analysis: Robustness properties and new paleoclimate applications", *Signal Process.*, **93**(5), 1079-1094.

https://doi.org/10.1016/j.sigpro.2012.11.029
Wang, C., Ren, W.X., Wang, Z.C. and Zhu, H.P. (2013), "Instantaneous frequency identification of time-varying structures by continuous wavelet transform", *Eng. Struct.*, **52**(9), 17-25. https://doi.org/10.1016/j.engstruct.2013.02.006
Zhu, J., Wang, C., Hu, Z.Y., Kong, F.R. and Liu, X.C. (2015), "Adaptive variational mode decomposition based on artificial fish swarm algorithm for fault diagnosis of rolling bearings", *J. Mech. Eng. Sci.*, **231**(4), 635-654. https://doi.org/10.1177/0954406215623311

CC